Proceedings of the ASME 2013 Conference on Smart Materials, Adaptive Structures and Intelligent Systems
SMASIS2013
September 16-18, 2013, Snowbird, Utah, USA

SMASIS2013-3272

A COMPLIANT ANKLE-FOOT ORTHOSIS (AFO) BASED ON MULTI-AXIAL LOADING OF SUPERELASTIC SHAPE MEMORY ALLOYS

Morteza GorzinMataee
Graduate Research Assistant
morteza.gorzinmataee@rockets.utoledo.edu

Masood Taheri Andani
Graduate Research Assistant
masood.taheriandani@rockets.utoledo.edu

Mohammad Elahinia
Associate Professor
mohammad.elahinia@utoledo.edu

Dynamic and Smart Systems Laboratory, University of Toledo, 2801 West Bancroft St. Toledo, OH 43606

ABSTRACT

This paper presents a novel actuation solution to address the drop foot disorder. The proposed actuator consists of a superelastic Nitinol rod with a variable torsional stiffness that is adjusted by the controlled application of an axial load. The superelastic SMA element enables the AFO to provide sufficient torque during dorsiflexion to raise the foot. The provided torque at the ankle joint assists the patient in walking more naturally and subsequently prevents further issues such as muscle atrophy.

By appraising experimental data of the human gait, ankle stiffness is assessed in order to compare ankle behavior for various walking speeds during the swing phase. The adjustable compliance concept for the AFO is then explained, followed by a description of the actuation mechanism and complex loading configuration. Numerical modeling is also presented for the superelastic element of the AFO under specified multiaxial torsion-tension loading. Simulations are performed in MATLAB and variable stiffness results are compared with experimental data for verification.

INTRODUCTION

An Ankle Foot Orthosis (AFO) is a brace often used by drop foot patients with paretic ankle dorsiflexor muscles. Drop foot is a neuromuscular disorder that deteriorates the patients' walking ability to raise their foot up. That happens due to muscle function insufficiency at the ankle joint. Drop foot might be a temporary or permanent weakness in the affected limb. Without treatment, it may develop into a severe disorder, capable of damaging other limbs and causing a permanent abnormal gait. A controlled force applied by the AFO device prevents the foot drop and foot slap defects during swing phase of the gait. This is intended to improve patients' walking pattern and normalize the gait [1, 2].

A passive AFO assists the ankle during the swing phase of the gait. It acts like a torsional spring, recovering the foot deflection by providing an external force. These AFOs, however, may not adjust to various walking speeds and stride patterns. Furthermore, the orthosis' excessive plantarflexion resistance could prevent stable ankle movement. It is therefore desirable for the AFO to have adjustable stiffness [3].

There are different concepts of powered orthotic devices employing hydraulic, pneumatic, magnetic and electric actuation mechanisms for producing assistive and resistive movement. MIT's series elastic [4] and Arizona State's robotic tendon [5] are two of the most popular active assistive AFOs. Osaka University's AFO [6], which utilizes a magneto rheological (MR) damper is an active device based on resistive motion. The problems with these devices are the bulky structure and tethered source of power that makes the device uncomfortable for daily usage. A portable powered ankle-foot orthosis (PPAFO) was developed at the University of Champaign Illinois [7] using a pneumatic actuator, a CO2 power source, and an onboard controller and sensors. Although this AFO presents an untethered, controllable device, performance of the device as a sustained rehabilitation tool for daily wearing depends on future studies and improving the endurance of the AFO.

A novel actuation design based on thermo-mechanical properties of shape memory alloys was proposed in Dynamic and Smart Systems Laboratory at the University of Toledo [8].We investigated combinations of superelastic and shape memory wires to develop an active actuator for AFOs. The limitation for this design was heating and cooling of the shape memory element due to the limited response time of the actuator in comparison to the walking cycle time. A new generation of SMA AFOs consisting of parallel superelastic wires subjected to tensile loading was also developed [9]. In this design SMA wires elongated during the powered plantarflexion, which assist the foot in dorsiflexion during the swing phase.

In this paper we have investigated an active AFO with adjustable torsional stiffness. An SMA rod is employed in parallel with the ankle joint. This concept is based on specified multi-axial loading patterns of SMA which provides complex output profiles according to the application requirements. A gait analysis is carried out to extract experimental data for ankle stiffness during the swing phase of the gait where drop foot should be addressed. The concept is finally evaluated by comparing the numerical results against the experimental gait data for the ankle stiffness.

GAIT ANALYSIS

Stance and swing are the two main phases of the gait cycle. During stance, the foot supports the whole body, which is comprised of three separate sub-phases. At the beginning, both feet are in contact with the ground, then during single limb stance the left foot swings and the right foot touches the ground. This is followed by double support, when both feet are in full contact with the ground. However, during swing phase, one foot swings forward with no ground contact.

A complete gait cycle for one leg, as shown in Figure 1, includes the following events:

I- Heel strike: The gait starts with an initial contact, which occurs at the moment the foot touches the ground

II- Foot-flat: Full soul contact, which lasts 10% of the whole cycle

III- Mid-stance: Begins when the opposite foot finishes the stance phase and starts swing. This event takes about 20% of the whole gait

IV- Heel-off: Occurs during terminal stance when the heel leaves the ground, for 20% of the cycle

V- Toe-off: Occurs during terminal stance when the toes leave the ground and complete foot-ground separation occurs. This is usually 10% of the cycle

VI- Swing acceleration: After toe-off, the hip accelerates the leg for about 10% of the gait in initial swing

VII- Mid-swing: Occurs when the active foot is in dorsiflexion and the opposite foot is in mid-stance. It goes on for about 15% of the cycle

VIII-Deceleration: Occurs when muscles decelerate the foot in order to prepare it for initial contact at heel strike, which lasts for 15% of gait in terminal swing

These eight events describe the whole gait cycle. More information about the human gait phases and events are available in [10].

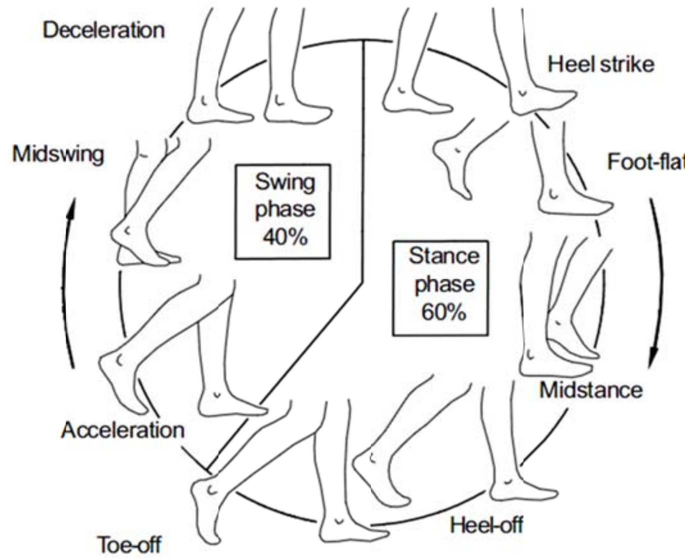

FIGURE 1: SEGMENTED CYCLE DIAGRAM OF HUMAN GAIT MAIN EVENTS AND PHASES [10]

Ankle joint stiffness is the resistance of the ankle joint in response to an applied ankle rotation during gait [11]. Investigations of the swing phase of the gait identify the drop foot disability as one of the most significant issues during patients' walking. By adjusting ankle joint stiffness during swing, we can achieve a functional gait cycle with the AFO.

From experimental data published by Gabriel et al. [12] and Hansen et al. [13], data of ankle moment-angle are extracted for a healthy foot at normal walking speed. For various speed conditions, published data by Hansen et al. [14] and Lelas et al. [14] are used to predict the desired behavior of the device for different ankle stiffness. Drop foot gait was investigated by Bhadane [8]. From the referenced, experimental data for healthy and drop foot behavior in various speed conditions are plotted for the swing phase of the gait (Figure 2-4). In these figures, the blue data points are experimental data. Linearized 1st and 2nd order polynomial curves are shown in green and red, respectively, to compare the slopes of ankle stiffness. It's clear from the graphs that the 2nd order polynomial represents the best fit for the data.

In Figure 2, the torque-rotation profile of the ankle for a fast gait is presented for swing. Clearly from this curve, the ankle behaves like a soft nonlinear torsional spring. Figure 3 shows the ankle torque-rotation for normal walking during the swing. The slow walking ankle behavior is presented in Figure 4, which resembles a stiffer torsional spring.

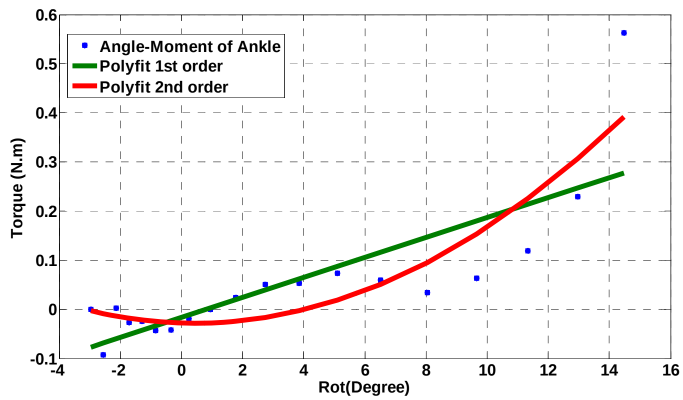

FIGURE 2: ANKLE TORQUE VS. ROTAION FOR FAST WALKING SPEED IN SWING PHASE OF THE GAIT

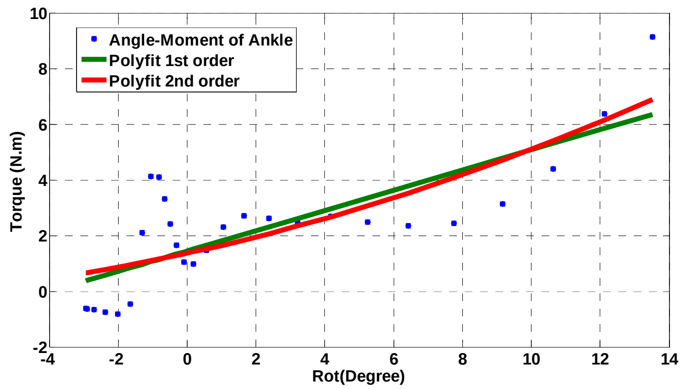

FIGURE 3: ANKLE TORQUE VS. ROTAION FOR NORMALWALKING SPEED IN SWING PHASE OF THE GAIT

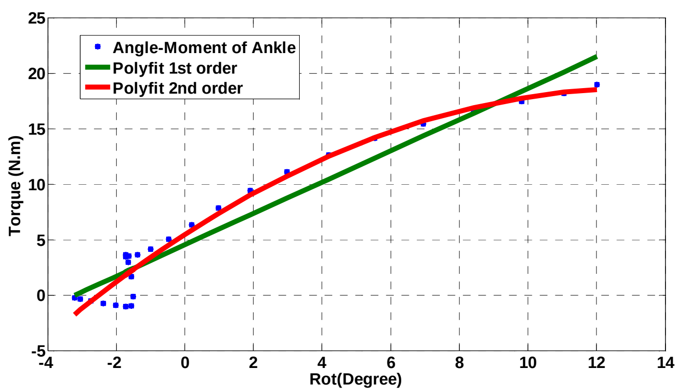

FIGURE 4: ANKLE TORQUE VS. ROTAION FOR SLOW WALKING SPEED IN SWING PHASE OF THE GAIT

The2nd order polynomial curves of ankle moment-rotation for different walking speeds are compared in Figure 5. As implied from this plot, the ankle stiffness significantly changes by the speed. In slow walking, the ankle behaves much stiffer than for faster speeds.

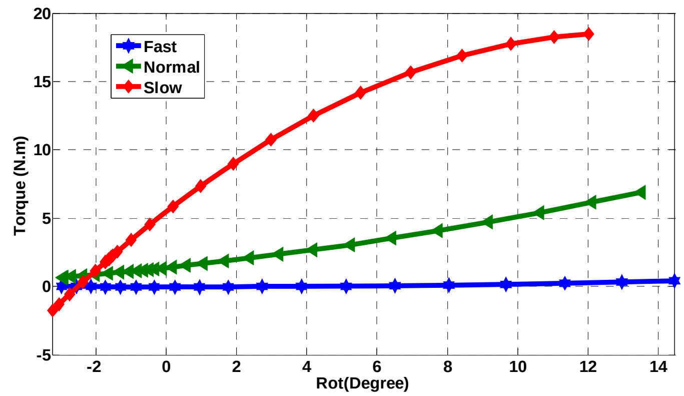

FIGURE 5: COMPARISONSFOR 2nd ORDER POLYNOMIAL ANKLE STIFFNESS IN VARIOUS SPEEDSFOR THE SWING

ADJUSTABLE COMPLIANCE CONCEPT

The idea is based on providing an adjustable compliant mechanism for patients who need assistance to achieve a healthy walking pattern. It is known that the ankle stiffness behavior for a healthy foot and a drop foot patient are not identical. Adding a device in series or parallel with the ankle, or a combination of these two, provides a flexible source to adjust the ankle stiffness and help the foot act normal. In a parallel connection of the element to the ankle, the element has the same rotation as the ankle. While in a series connection, a similar moment is applied to the element and the ankle. For series and parallel patterns, the desired stiffness for the device is:

$$K_e(parallel\ pattern) = K_{ha} - K_{da} \tag{1}$$

$$K_e(series\ pattern) = \left(\frac{1}{K_{ha}} - \frac{1}{K_{da}}\right)^{-1} \tag{2}$$

where K_e is the desired stiffness of the AFO device ,K_{ha} is the stiffness for the healthy ankle and K_{da} is the stiffness for the drop foot ankle.

It is considered that the element to be connected in parallel pattern to the ankle and to have the same deflection rather than similar moment as shown in Figure 6.

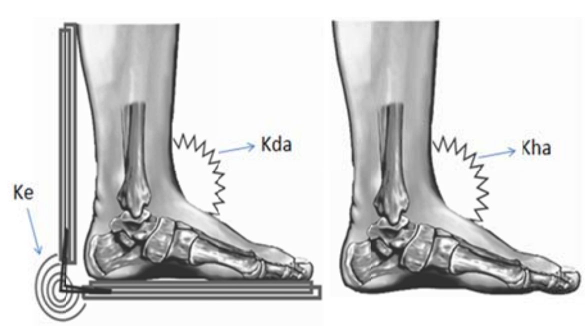

FIGURE 6: ANKLE STIFNESS FOR THE DEVICE, DROP FOOT ANKLE AND HEALTHY ANKLE

A superelastic SMA element attached to the ankle as a compliance will timely store and release energy during a walking gait. However, uncontrolled energy storage and return of the prosthetic element will decline the activity of the muscle that is responsible for propulsion in the gait. Also, this behavior is more observable in compliant ankles [15].

Therefore, a mechanism must be designed, either passive or active, that can regulate the ankle compliance.

AFO ACTUATION MECHANISM

In order to achieve required stiffness for the AFO, a novel concept for an actuator mechanism is proposed, as depicted in Figure 7. This mechanism is aimed at assisting dorsiflexion during the swing phase by releasing energy stored during plantarflexion in the terminal stance phase. A primary goal of the design is to reproduce a variable stiffness profile by manipulating the system using a linear actuator. A superelastic SMA rod used as a variable stiffness element, which is attached to the ankle in series by means of an AFO. Ankle rotation provides torsional loading for the element and the linear actuator provides the axial loading. This combination of torsion-tension loading offers the SMA element adjustable compliance which is controllable by loading and timing of the linear actuator. This system works as an adaptive structure which could actively be adjusted to various walking speeds. However, it would be a passive device if the linear actuator is excluded from the configuration.

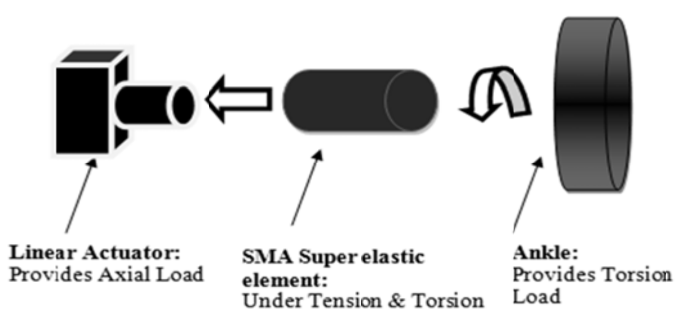

FIGURE 7: TORSION-TENSION LOADING APPLIEDTO SMA ELEMENT IN ORDER TO PROVIDEAN ADJUSTABLE COMPLIANT ACTUATOR FOR CONTROLLINGANKLE STIFFNESS

NUMERICAL MULTI AXIAL LOADING MODEL FOR THE AFO SMA ELEMENT

The model used in this work is an extension of the models presented by Boyd and Lagoudas [16] and Qidwai and Lagoudas [17].

The following classic decomposition of the total strain is assumed as the first step in developing the constitutive model:

$$\varepsilon = S\colon\sigma + \alpha(T - T_0) + \varepsilon^t \tag{3}$$

Where S, σ, α, T and T_0 are the effective compliance tensor, Cauchy stress tensor, effective thermal expansion coefficient tensor, temperature and reference temperature, respectively. The sign (:) indicates double dot product operation between two tensors. ε^t is the inelastic strain caused by the martensitic transformation in the material. In the implemented model, it is assumed that the evolution of the transformation strain tensor is proportionally dependent on the change in the martensite volume fraction shown by $\dot{\xi}$. This relation is defined through the following expression:

$$\dot{\varepsilon}\colon\Gamma = \Lambda\dot{\xi} \tag{4}$$

Where the newly defined transformation identity tensor is 5th order and is defined as:

$$\Gamma = \mathrm{diag}(1,1,1,k_s k_e, k_s k_e, k_s k_e) \tag{5}$$

The direction of the transformation strain is dictated by the transformation tensor Λ and is assumed to be:

$$\Lambda = \begin{cases} \frac{3}{2}H\Omega\colon\frac{\acute{\sigma}}{\bar{\sigma}} & ,\dot{\xi} > 0 \\ \Gamma\colon\frac{\varepsilon^{t-r}}{\xi^{t-r}} & ,\dot{\xi} < 0 \end{cases} \tag{6}$$

Where H, $\acute{\sigma}$ and$\bar{\sigma}$ are the maximum axial transformation strain, deviatoric stress tensor and effective stress, respectively. ε^{t-r} and ξ^{t-r} are the transformation strain and martensitic volume fraction at the reversal point, which represent the state of transformation at the end of loading. Ω is the effective identity stress tensor:

$$\Omega = \mathrm{diag}(1,1,1,k_s^2,k_s^2,k_s^2) \tag{7}$$

To transformation, there is an inequality derived from the second law of thermodynamics which should be satisfied in all material states. This inequality is defined as:

$$(\sigma, T, \xi) \leq 0 \rightarrow \begin{cases} \Phi = 0 & \text{if } \dot{\xi} \neq 0 \\ \Phi < 0 & \text{if } \dot{\xi} = 0 \end{cases} \tag{8}$$

The 3D model predicts the mechanical response of superelastic NiTi for various loading conditions including proportional and non-proportional tension-torsion patterns at different temperature.

NUMERICAL RESULTS

Numerical model for SMA element is implemented in MATLAB. SMA element is designed for the AFO is a superelastic NiTi rod with a diameter of 6.4 mm and total length of 25 mm. Material properties used in the numerical investigation are presented in Table1.

TABLE 1: ELEMENT MATERIAL PROPERTIES

EA	50.0e3 (Mpa)
EM	10.0e3 (Mpa)
Mf	241.0 (K)
Ms	258.0 (K)
Af	283.0 (K)
As	273.0 (K)
CM	7.5 (Mpa/K)
CA	8.3 (Mpa/ K)
ν	0.3
H	0.03

The loading condition is defined by the following steps:
Step 1: An axial load is applied by the linear actuator during mid-stance for 20% of the gait cycle.
Step 2: loading torsional load is applied by means of the ankle rotation during terminal stance for 20% of the gait cycle.
Step 3 and Step 4: The axial and torsional loads are recovered during the swing phase for about 35% of gait cycle.
Torsional loading is applied by the ankle during waking, while the axial loading is controlled externally. By controlling the axial displacement through the actuator, different stiffness curves are achievable. Two variables are defined in order to control the system. The first is the amount of pretension in SMA element, which is applied in step 1 as a linear displacement. The second variable is the portion of axial recovery during swing, which is determined to be the amount of displacement that is recovered in step 4 at mid-swing to the total amount of displacement in step 3 and 4. By playing with these two variables we can then achieve desired stiffness curves. Figure 8 shows how the SMA stiffness curves are numerically adjusted to fit into the experimental ankle stiffness. The red curve is the experimental data for normal walking speed during swing phase. The blue and the green curves are the 1st and 2nd order polynomial curve fits. The black curve shows loading and unloading behavior of superelastic SMA element which is loaded during the stance phase and unloaded during the swing. The unloading curve is supposed to fit to experimental data as it's shown in Figure 8.

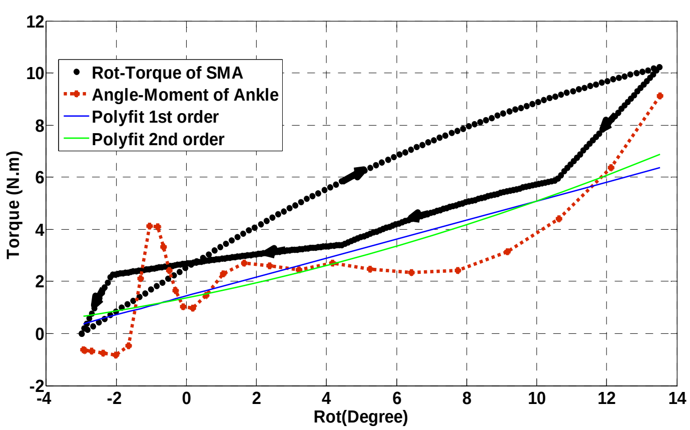

FIGURE 8: DESIRED STIFFNESS CURVE AT SWING BY APPLYING MULTI AXIAL LOADING ON SMA ELEMENT

By adjusting pre-tension of the amount of axial recovery, according to Table 2, desired stiffness for three different gait speeds of slow, normal and fast are attained. Results are presented in Figure 9 for the MATLAB modeling of the SMA rod under induced tension and torsion loading conditions.

TABLE 2: VARIABLE ADJUSTMENT FOR DIFFERENT GAIT SPEEDS

Gait Speed	Pre-tension	Portion of axial recovery
Slow Speed	1 mm	0 %
Normal Speed	0.5 mm	65 %
Fast Speed	1.75 mm	50 %

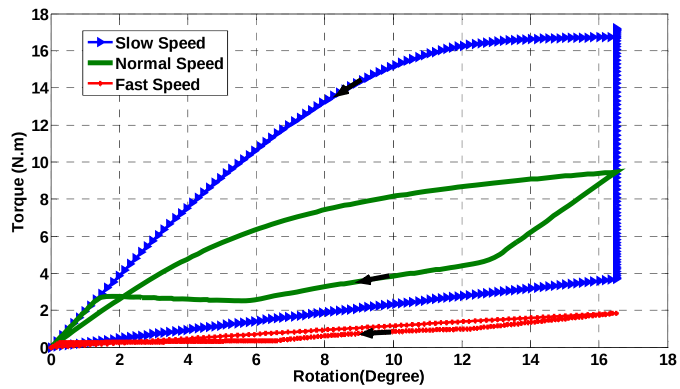

FIGURE 9: MATLAB MODELING RESULT FOR DESIRED STIFFNESS CURVES AT VARIOUS SPEED CONDITION

CONCLUSION

A novel adjustable compliant AFO concept is proposed in this paper. Based on detailed gait analyses from experimental data, stiffness variation is determined in different walking speeds through the swing phase of the gait. The actuation mechanism is explained by prescribing a superelastic element under multiaxial loading conditions, including rotational deflection provided by the ankle movement and linear displacement provided by a linear actuator. An analytical model for SMA tension-torsion loading is then explained and implemented. A numerical study was accomplished in MATLAB. These were used to find the effect of the actuator loading condition on ankle stiffness behavior for different walking speeds. Results that verify the performance of the concept were then compared and reported. It's inferable from the numerical results that nonlinear ankle stiffness is accurately attainable by tuning the loading-unloading variables, which are SMA pre-tension magnitude during mid-stance and the magnitude of axial load recovery during swing. By adjusting these two parameters, stiffness curves for different walking speeds are achieved. Results demonstrate that by increasing the portion of axial recovery and by increasing the pre-tension at the same time, we reach a softer behavior which is desired for faster walking speeds. Furthermore, by increasing the portion of axial recovery and decreasing the pre-tension, behavior required for normal walking speed is obtainable. Moreover, by simultaneously decreasing the portion of axial recovery and pre-tension, a stiffer behavior desired for slow walking speed is achievable. This approach may be extended to more complex loading conditions to predict more complicated gait adventures like severe speed changes or uphill and downhill walking.

REFERENCES

[1] Johanna F. Geboers, Maarten R. Drost, Frank Spaans, Harm Kuipers, Henk A. Seelen,, 2002, "Immediate and Long-Term Effects of Ankle-Foot Orthosis on Muscle Activity During Walking: A Randomized Study of Patients With Unilateral Foot Drop" *Archives of Physical Medicine and Rehabilitation*

[2] Wu, Kent. K.,1990, "Foot orthoses: Principles and clinical applications"*Baltimore: Wlliams & Wilkins*

[3] MinalBhadane, Mohamed Samir Hefzy, Charles Armstrong, Mohammad Elahinia, 2011, " An Automated Testing Assembly for characterizing Stiffness of AN Ankle Foot Orthosis" *ASME 2011 Conference on Smart Materials, Adaptive Structures and Intelligent Systems*

[4] Blaya, J.A., Herr, H., 2004, "Adaptive Control of a Variable Impedance Ankle Foot Orthosis to assist Drop Foot Gait" *IEEE Transactions on Neural Systems and Rehabilitation Engineering,* **12** (1), pp. 24-31.

[5] Boehler, A.W., et al., 2008, "Design, implementation and test results of a robust control method for a powered ankle foot orthosis (AFO)" *IEEE International Conference on Robotics and Automation*

[6] Furusho, J., et al., 2007, "Development of shear type compact MR brake for the intelligent ankle footorthosis and its control" *Research and development in NEDO for practical application of human support robot. IEEE 10th International Conference on Rehabilitation Robotics, 2007. Noordwijk, the Netherlands*

[7] Kenneth Alexander Shorter, 2011, "The Design And Control Of Active Ankle-Foot Orthoses" *Submitted in partial fulfillment of the requirements for the degree of Doctor of Philosophy in Mechanical Engineering in the Graduate College of the University of Illinois at Urbana-Champaign*

[8] Minal Bhadane, 2012, "Towards a Shape Memory Alloy Variable Stiffness Ankle Foot Orthosis" *Submitted to the Graduate Faculty as partial fulfillment of the requirements for The Doctor of Philosophy Degree in Engineering, the University of Toledo*

[9] Liberty Deberg, 2012, "A Fast Actuator Using Shape Memory Alloys for An Ankle Foot Orthosis", *Dissertation submitted to The University of Toledo, Ecole des Sciences et Technologies de l'Ingénieur de Nancy*

[10] Christopher L Vaughan, Brian L Davis, Jeremy C O'Conor, 1992, "Dynamics of Human Gait"*Kiboho Publishers, South Africa*

[11] R.B. Davis and P.A. DeLuca, 1996, "Gait characterization via dynamic joint stiffness",*Gait Posture*, **4**, pp. 224–231

[12] Ronaldo C. Gabriela, Joa˜oAbrantesb, Kevin Granatac, Jose´Bulas-Cruzd, Pedro Melo-Pintod, Vitor Filipe, 2008, "Dynamic joint stiffness of the ankle during walking: Gender-related differences"*R.C. Gabriel et al. / Physical Therapy in Sport,* **9**, pp. 16–24

[13] Andrew H. Hansen, Dudley S. Childress, Steve C. Miffb, Steven A. Gard, Kent P. Mesplay, 2004 "The human ankle during walking: implications for design of biomimetic ankle prostheses"*A.H. Hansen et al. / Journal of Biomechanics,* **37**, pp. 1467–1474

[14] Jennifer L. Lelas, Gregory J. Merriman, Patrick O. Riley, D. Casey Kerrigan, 2003, "Predicting peak kinematic and kinetic parameters from gait speed"*J.L. Lelas et al. / Gait and Posture,* **17**, pp. 106_112

[15] Jessica D. Ventura, Glenn K. Klute, Richard R. Neptune, 2011, "The effect of prosthetic ankle energy storage and return properties on muscle activity in below-knee amputee walking" *J.D. Ventura et al. / Gait & Posture,* **33**, pp. 220–226

[16] Boyd, J., and Lagoudas, D., 1996, "A thermodynamic constitutive model for the shape memory alloy materials. parti. the monolithic shape memory alloy",*International Journal of Plasticity,* **12**, pp. 805–842

[17] Qidwai, M. A., and Lagoudas, D. C., 2000, "On thermomechanics and transformation surfaces of polycrystalline Niti shape memory alloy material", *International Journal of Plasticity,* **16**, pp. 1309–1343